Molecular Pharmacology Fast Forward. Published on November 29, 2010 as doi:10.1124/mol.110.068551
This article has not been copyedited and formatted. The final version may differ from this version.

MOL #68551

ROS-dependent apoptosis by gugulipid extract of *Ayurvedic* medicine plant *Commiphora mukul* in human prostate cancer cells is regulated by c-JUN N-terminal kinase*

Dong Xiao, Yan Zeng, Lakshmi Prakash, Vladmir Badmaev, Muhammed Majeed and Shivendra V. Singh

Department of Pharmacology & Chemical Biology, University of Pittsburgh School of Medicine (D.X., S.V.S.) and University of Pittsburgh Cancer Institute (D.X., S.V.S., Y.Z.), Pittsburgh, PA. Sabinsa Corporation (L.P., V.B., M.M.), Piscataway, NJ.

Molecular Pharmacology Fast Forward. Published on November 29, 2010 as DOI: 10.1124/mol.110.068551
This article has not been copyedited and formatted. The final version may differ from this version.

MOL #68551

Running head: JNK activation in gugulipid-induced apoptosis

Correspondence author: Dr. Dong Xiao, 2.32b Hillman Cancer Center Research Pavilion, 5117 Centre Avenue, Pittsburgh, PA 15213. Phone: 412-623-3262; Fax: 412-623-7828; E-mail: dongx@upmc.edu.

The number of text pages: 29

The number of tables: 0

The number of figures: 6

The number of references: 40

The number of words in the abstract: 239

The number of words in the introduction: 599

The number of words in the discussion: 1083

ABBREVIATIONS: CDCFDA, (5-(and-6)-carboxy-2',7'-dichloroluorescein diacetate, succinimidyl ester; HE, hydroethidine; PARP, poly-(ADP-ribose)-polymerase; DMSO, dimethyl sulfoxide; PBS, phosphate buffered saline; BSA, bovine serum albumin; DCF, 2',7'-dichlorodihydrofluorescein; JNK, c-Jun N-terminal kinase; MAPK, mitogen-activated protein kinase; JNKK2, JNK kinase 2; PrEC, normal human prostate epithelial cell line.

Molecular Pharmacology Fast Forward. Published on November 29, 2010 as DOI: 10.1124/mol.110.068551
This article has not been copyedited and formatted. The final version may differ from this version.

Abstract

Gugulipid (GL), extract of Indian Ayurvedic medicinal plant *Commiphora mukul*, has been used to treat a variety of ailments. We now report anti-cancer effect and mechanism of GL against human prostate cancer cells. Treatment with GL significantly inhibited viability of human prostate cancer cell line LNCaP (androgen-dependent) and its androgen-independent variant (C81) with an IC_{50} ~ 1 μM (24 h treatment) at pharmacologically relevant concentrations standardized to its major active constituent z-guggulsterone. The GL-induced growth inhibition correlated with apoptosis induction as evidenced by an increase in cytoplasmic histone-associated DNA fragmentation and sub-G_0/G_1DNA fraction, and cleavage of poly-(ADP-ribose)-polymerase (PARP). The GL-induced apoptosis was associated with reactive oxygen species (ROS) production and c-Jun NH_2-terminal kinase (JNK) activation. The induction of proapoptotic Bcl-2 family proteins Bax and Bak and a decrease of antiapoptotic Bcl-2 protein Bcl-2 were observed in GL-treated cells. SV40 immortalized mouse embryonic fibroblasts derived from Bax-Bak double knockout mice were significantly more resistant to GL-induced cell killing compared with wild type cells. It is interesting to note that a representative normal prostate epithelial cell line PrEC was relatively more resistant to GL-mediated cellular responses compared with prostate cancer cells. The GL treatment caused activation of JNK that functioned upstream of Bax activation in apoptosis response. The GL-induced conformational change of Bax and apoptosis were significantly suppressed by genetic suppression of JNK activation. In conclusion, the present study indicates that ROS-dependent apoptosis by GL is regulated by JNK signaling axis.

Molecular Pharmacology Fast Forward. Published on November 29, 2010 as DOI: 10.1124/mol.110.068551
This article has not been copyedited and formatted. The final version may differ from this version.

Introduction

Novel strategies for prevention of prostate cancer are highly desirable because prostate cancer continues to be leading cause of cancer-related deaths among men in the United States (Jemal et al., 2009; Whittemore et al., 1995). Prostate cancer is usually diagnosed in the sixth or seventh decades of life, which allows a large window of opportunity for intervention to prevent or slow progression of the disease (Whittemore et al., 1995; Gilligan and Kantoff, 2002). Thus, clinical development of agents from natural products that are relatively safe but can delay onset and/or progression of human prostate cancer is highly desirable.

Gugulipid (GL), extract of *Commiphora mukul, has* been safely used in the Indian Ayurvedic medicine practice for treatment of different ailments (Shishodia et al, 2008; Urizar and Moore, 2003; Badmaev et al., 2003). Several products of standardized formulations of *Commiphora mukul* are already in human use as cholesterol-lowering agents (Shishodia et al, 2008; Urizar and Moore, 2003; Badmaev et al., 2003). The z- and E-forms of guggulsterone (4,17(20)-pregnadie-3, 16-dione) have been identified as major active components of GL, which has been used in many clinical trials that have focused on its cholesterol-lowering effect (Shishodia et al, 2008; Urizar and Moore, 2003; Badmaev et al., 2003). Although the antitumor activity of GL has not been studied yet, the studies, including ours, have shown that z-guggulsterone (z-Gug) inhibits proliferation, induces apoptosis; and suppresses angiogenesis as well as the invasion and metastasis of cancer cells (Shishodia et al, 2008; Urizar and Moore, 2003; Badmaev et al., 2003; Gujral et al., 1960; Sinal and Gonzalez, 2002; Shishodia and Aggarwal, 2004; Samudio et al., 2005; Ichikawa and Aggarwal, 2006; Cheon et al., 2006; Xiao and Singh, 2008; Singh et al., 2005a, 2007; Urizar et al., 2002; Cui et al., 2003; Wu et al, 2002). Apoptosis induction by Gug has been reported in leukemia, multiple myeloma, melanoma, head

Molecular Pharmacology Fast Forward. Published on November 29, 2010 as DOI: 10.1124/mol.110.068551
This article has not been copyedited and formatted. The final version may differ from this version.

and neck, lung, ovarian, prostate and breast cancer cells (Sinal and Gonzalez, 2002; Shishodia and Aggarwal, 2004; Samudio et al., 2005; Ichikawa and Aggarwal, 2006; Cheon et al., 2006; Xiao and Singh, 2008; Singh et al., 2005a, 2007; Urizar et al., 2002; Cui et al., 2003; Wu et al, 2002). We have shown previously that z- and E-Gug inhibit growth of PC-3, DU145 and LNCaP human prostate cancer cells in culture by causing apoptosis (Singh et al., 2005a, 2007). Interestingly, a normal prostate epithelial cell line (PrEC) is significantly more resistant to growth inhibition and apoptosis induction by z-Gug compared with prostate cancer cells (Singh et al., 2005a, 2007). The z-Gug-induced cell death in PC-3 cells was not influenced by Bcl-2 protein level but correlated with induction of proapoptotic multidomain Bcl-2 family members Bax and Bak and activation of caspases (Singh et al., 2005a). The z-Gug-induced apoptosis in human prostate cancer cells was initiated by reactive oxygen intermediate-mediated activation of c-Jun NH_2-terminal kinase (Singh et al., 2007). Our previous study demonstrated that z-Gug and E-Gug inhibit angiogenic features (capillary-like tube formation and/or migration) of human umbilical vein endothelial cells (HUVEC) and DU145 human prostate cancer cells *in vitro* at pharmacologically relevant concentrations (Xiao and Singh, 2008). Furthermore, oral gavage of 3 µmol z-Gug to male nude mice (five times per week) inhibits *in vivo* angiogenesis (Xiao and Singh, 2008).

Based on these data, we hypothesized that GL might be more effective apoptosis induced in prostate cancer cells because it contains a number of steroids, including the two isomers z- and E-Gugs (Shishodia et al, 2008; Urizar and Moore, 2003; Badmaev et al., 2003). In present studies, we tested this hypothesis by examining the effect of GL standardized to z-Gug.

Molecular Pharmacology Fast Forward. Published on November 29, 2010 as DOI: 10.1124/mol.110.068551
This article has not been copyedited and formatted. The final version may differ from this version.

Materials and Methods

Reagents. GL, derived from the gum guggul resin (gum guggul) produced in the soft bark ducts of the *Commiphora mukul* tree, is a registered product of Sabinsa Corporation (Registration date: July 21, 1992; US Patent# 6436991 B1). A manufacturing flow chart for gum guggul resin to GL was described by us previously (Badmaev et al., 2003). Standardization of GL was performed by high-performance liquid chromatography (HPLC) and found to contain ~3.75% z-Gug (Badmaev et al., 2003). The GL was stored at 4^0C and found to be stable for at least 6 months. The *z*-Gug was from Steraloids (Newport, RI). Reagents for cell culture including medium, penicillin and streptomycin antibiotic mixture, and fetal bovine serum were purchased from Invitrogen (Carlsbad, CA). The hydroethidine (HE) and (5-(and-6)-carboxy-2',7'-dichloroluorescein diacetate, succinimidyl ester (CDCFDA) were from Molecular Probes (Eugene, OR). The ELISA kit for quantitation of cytoplasmic histone-associated DNA fragmentation was from Roche Diagnostics (Mannheim, Germany). The p38 MAPK and p44/p42 MAPK (Erk1/2)-targeted small interfering RNA (siRNA) were from Cell Signaling Technology (Danvers, MA). The anti-Bax (6A7) monoclonal antibody was from Pharmingen (Palo Alto, CA), antibodies against Bax (polyclonal anti-Bax), Akt, phosphor-Akt and phosphor-mTOR were from Cell Signaling Technology, the antibody against α-Tubulin was from Sigma, the antibodies specific for detection of poly-(ADP-ribose)-polymerase (PARP), Bak, total JNK, phospho-(Thr^{183}/Tyr^{185})-JNK, total p38 MAPK, phospho-(Tyr^{182})-p38 MAPK, extracellular-signal-related kinase 1/2 (ERK1/2), phospho-ERK1/2 and phospho-(Ser63/730)-c-Jun were from Santa Cruz Biotechnology (Santa Cruz, CA), the anti-Bcl-2 antibody was from DAKOCytomation (Carpinteria, CA), and anti-actin antibody was from Oncogene Research

Molecular Pharmacology Fast Forward. Published on November 29, 2010 as DOI: 10.1124/mol.110.068551
This article has not been copyedited and formatted. The final version may differ from this version.

Products (San Diego, CA). *N*-acetyl-L-cysteine (NAC) was obtained from Sigma-Aldrich (St. Louis, MO).

Cell culture and cell survival assays. Monolayer cultures of LNCaP and C81 cells were maintained in RPMI1640 medium supplemented with 10% (v/v) FBS, 10 mM HEPES, 1 mM sodium pyruvate, 0.2% glucose and antibiotics. Normal prostate epithelial cell line PrEC (Clonetics, San Diego, CA) was maintained in PrEBM (Cambrex, Walkersville, MD). The MEFs derived from wild type, and Bax-Bak double knockout (DKO) mice and immortalized by transfection with a plasmid containing SV40 genomic DNA were generously provided by the late Dr. Stanley Korsmeyer (Dana-Farber Cancer Institute, Boston, MA), and maintained as described by us previously (Singh et al., 2005a). Each cell line was maintained in an atmosphere of 95% air and 5% CO_2 at 37^0C. The effect of GL and z-Gug on cell viability was determined by (a) colonogenic survival assay and (b) trypan blue dye exclusion assays as described by us previously (Xiao and Singh, 2007; Kim et al., 2007; Xiao et al., 2006a, 2008). For the colonogenic survival assay, cells (1.5×10^5) were plated in 6-well-plates for incubation overnight and then were treated with 0.1 % DMSO (control group) or 1, 2.5 and 5 μM GL for 24 h. The treated cells were re-seeded in 6-well plates (500 cells/well) in complete medium without drug. The medium were changed every two days. After culture 10 days, the cells were fixed and stained with 0.5 % crystal violet in 20% MeOH for colony counting.

Detection of apoptosis. Apoptosis induction was assessed by (a) analysis of cytoplasmic histone-associated DNA fragmentation, (b) flow cytometric analysis of cells with sub-G_0/G_1 DNA content following staining with propidium iodide and (c) immunoblotting analysis of cleavage of PARP as described by us previously (Kim et al., 2007; Xiao et al., 2006a).

Molecular Pharmacology Fast Forward. Published on November 29, 2010 as DOI: 10.1124/mol.110.068551
This article has not been copyedited and formatted. The final version may differ from this version.

Immunoblotting. The cells were treated with GL and were lysed as described by us previously (Xiao and Singh, 2008; Singh et al., 2007). The lysate proteins were resolved by 6-12.5% sodium dodecyl sulfate polyacrylamide gel electrophoresis and transferred onto membrane. Immunoblotting was performed as described by us previously (Xiao and Singh, 2008; Singh et al., 2007). The blots were stripped and re-probed with anti-actin antibody to correct for differences in protein loading. Change in protein level was determined by densitometric scanning of the immunoreactive band and corrected for actin loading control. Immunoblotting for each protein was performed at least twice using independently prepared lysates to ensure reproducibility of the results.

ROS generation assay. Intracellular ROS generation was measured by flow cytometry following staining with HE and CDCFDA essentially as described by us previously (Xiao et al., 2008). Briefly, 2×10^5 cells were plated in 60-mm culture dishes, allowed to attach by overnight incubation, and exposed to DMSO (control) or desired concentration of GL for specified time intervals. The cells were stained with 2 μM HE and 5 μM CDCFDA for 30 min at 37°C. The cells were collected and the fluorescence was measured using a Coulter Epics XL Flow Cytometer. In some experiments, cells were pretreated for specified time periods with NAC (10 mM) prior to GL exposure and analysis of ROS generation.

Genetic suppression of JNK in LNCaP cells. The LNCaP cells were transiently transfected with the plasmid encoding for catalytically inactive mutant of JNK kinase 2 [JNKK2(AA)], a generous gift from Dr. Michael Karin (University of California at San Diego, La Jolla, CA), or empty pcDNA3.1 vector as described by us previously (Xiao et al., 2008). The cells were then treated with DMSO (control) or 5 μM GL for specified time periods and processed for analysis

Molecular Pharmacology Fast Forward. Published on November 29, 2010 as DOI: 10.1124/mol.110.068551
This article has not been copyedited and formatted. The final version may differ from this version.

of DNA fragmentation, immunoblotting for phospho-JNK and phospho-c-Jun or conformational change of Bax.

Analysis of Bax conformation change. The cells were treated with 5 μM GL or DMSO (control) for specified time interval, and lysed using a solution containing 10 mM HEPES (pH 7.4), 150 mM NaCl, 1% CHAPS, and protease inhibitor cocktail. Aliquots containing 200 μg lysate proteins were incubated overnight at 4°C with 4 μg of anti-Bax 6A7 monoclonal antibody. Protein G-agarose beads (50 μl; Santa Cruz Biotechnology) were then added to each sample and the incubation was continued for an additional 2 h at 4°C. The immunoprecipitates were washed five times with lysis buffer and subjected to electrophoresis followed by immunoblotting using polyclonal anti-Bax antibody.

RNA interference of p38 MAPK and Erk1/2. The cells (1×10^5) were seeded in six-well plates and allowed to attach by overnight incubation. The cells were transfected with 200 nmol/L of control non-specific siRNA or p38 MAPK or Erk1/2-targeted siRNA using Oligofectamine (Invitrogen) according to the manufacturer's recommendations. Twenty-four hours after transfection, the cells were treated with DMSO (control) or 5 μmol/L GL for specified time period. The cells were collected, washed with phosphate-buffered saline (PBS), and processed for immunoblotting or analysis of cytoplasmic histone-associated DNA fragmentation as described by us previously (Xiao and Singh, 2010; 2007; Xiao et al., 2008).

Statistical analysis. Statistical significance of difference in measured variables between control and treated groups was determined by t-test or one-way ANOVA. Difference was considered significant at $P<0.05$.

Molecular Pharmacology Fast Forward. Published on November 29, 2010 as DOI: 10.1124/mol.110.068551
This article has not been copyedited and formatted. The final version may differ from this version.

Results

GL inhibited viability of human prostate cancer cells. The effect of GL standardized to z-Gug on cell viability was determined by the colonogenic assay. By following the colony formation assaying procedure, the cells were cultured for 10 days after 24 h exposure to GL and the colony formation (>50 cells/colony) were determined. The viability of both LNCaP and its androgen-independent variant C81 (Fig. 1A) was decreased significantly in a concentration-dependent manner with an IC_{50} of GL ~1 μM, which is at pharmacologically achievable concentrations (~3 μM, Verma et al., 1999). Growth inhibitory effect of GL was confirmed by trypan blue dye exclusion assay. Treatment with GL for 24 h resulted in a significant reduction in cell viability in both cells (Fig. 1B). Even though viability of LNCaP and C81 cells was also decreased in the presence of z-Gug (Fig. 1C), the GL appeared relatively more effective compared with z-Gug against both cell lines. Growth inhibitory effect of GL to the cancer cells was ~10-fold stronger compared with z-Gug (Fig. 1). The results indicate that the anti-cancer effect of GL against prostate cancer cells is most likely attributable to z-Gug as well as other constituent(s). Interestingly, a normal prostate epithelial cell line (PrEC) was significantly more resistant to growth inhibition by GL compared with prostate cancer cells (Fig. 1D). For instance, 2.5 μM GL, which inhibited viability of LNCaP and C-81 cells by about 50% (Fig. 1B), had minimal effect on PrEC cell viability (Fig. 1D). These data indicated that human prostate cancer cells, but not normal prostate epithelial cell PrEC, were sensitive to inhibition of cell viability by GL. Because the LNCaP and C81 cells exhibited comparable sensitivity, we can also conclude that androgen-responsiveness is not a critical factor in GL-mediated growth inhibition in prostate cancer cells.

Molecular Pharmacology Fast Forward. Published on November 29, 2010 as DOI: 10.1124/mol.110.068551
This article has not been copyedited and formatted. The final version may differ from this version.

GL-mediated suppression of cancer cell growth correlated with apoptotic DNA fragmentation. To gain further insights into the mechanism of GL-mediated inhibition of prostate cancer cell growth, we determined its effect on cytoplasmic histone-associated DNA fragmentation, a widely used technique for detection of apoptosis. The GL treatment resulted in a dose-dependent increase in cytoplasmic histone-associated DNA fragmentation in both LNCaP and C81 cells (Fig. 2A). Consistent with cell viability data (Fig. 1D), the PrEC cells were resistant to GL-induced cytoplasmic histone associated DNA fragmentation (2A). To conform the results of GL-induced apoptotic cell death, we further investigated whether GL treatment increased sub-G_0/G_1 DNA content. A dose-dependent increase in the proportion of cells with sub-G_0/G_1 content was observed in GL-treated LNCaP and C81 cells, but not in PrEC, compared with DMSO-treated control (Fig. 2B). Furthermore, an immunoreactive band corresponding to cleaved PARP was observed in both of cancer cells following treatment with GL (Fig. 2C). Taken together, these observations clearly indicated that antiproliferative effect of GL against prostate cancer cells was associated with apoptosis induction and this effect was selective for prostate cancer cells.

GL treatment caused ROS production in prostate cancer cells but not in a normal prostate epithelial cell PrEC. Our previous studies have shown that many natural products, such as, phenethyl isothiocyanate (Xiao and Singh, 2010; Xiao et al., 2006b), benzyl isothiocyanate (Xiao et al., 2006c, 2008), sulforaphane (Xiao et al, 2009; Singh et al., 2005a), diallyl trisulfide (Xiao et al., 2005b), and z-Gug (Singh et al., 2007), cause apoptosis through mediation of ROS. We tested whether GL-induced apoptosis was ROS-dependent using flow cytometry following staining with HE and CDCFDA. As can be seen in Figure 3A, GL-treated C81 cells exhibited a dose- and time-dependent increase in mean DCF fluorescence compared

Molecular Pharmacology Fast Forward. Published on November 29, 2010 as DOI: 10.1124/mol.110.068551
This article has not been copyedited and formatted. The final version may differ from this version.

with DMSO-treated (control) cells. For example, the DCF fluorescence in DCF in C81 cells treated for 30 min with 2.5 and 5 μM GL was increased by about 7.5- and 3.2-fold compared with control group (Fig. 3A). In time-course experiments, the ROS production was observed as early as 30 min and peaked between 1 h and 2 h post-exposure (Fig.3A). The LNCaP cells had almost a same response to GL treatment (Fig. 3B). It is important note that ROS generation was not determined in the normal prostate epithelial cell PrEC treated with (Fig.3C). These observations clearly indicated that GL treatment resulted in ROS production selectively in human prostate cancer cells.

NAC, an antioxidant, attenuated GL-induced ROS production and apoptosis in prostate cancer cells. Next, we designed experiments to determine whether GL-induced ROS generation and apoptotic cell death were attenuated by NAC, an antioxidant. The present results showed that pretreatment with NAC conferred significant protection against GL-induced ROS production and apoptosis in LNCaP cells (Fig. 3D).

Effect of GL treatment on levels of Bcl-2 family proteins. The Bcl-2 family proteins have emerged as critical regulators of mitochondria-mediated apoptosis by functioning as either promoters (e.g., Bax and Bak) or inhibitors (e.g., Bcl-2 and Bcl-xL) of the cell death process (Chao and Korsmeyer, 1998; Xiao et al., 2004, 2005c). We proceeded to test whether GL-induced apoptosis was regulated by Bcl-2 family proteins. The effect of GL treatment on levels of Bcl-2 family proteins in LNCaP cells was determined by immunoblotting and representative blots are shown in Figure 4A. The levels of multidomain proapoptotic proteins Bax and Bak were increased on treatment of LNCaP cells with GL. For example, GL-treated cells for 2-24 h resulted in an increase of 2-4 folds for Bax and about 2 folds for Bak protein expression (Fig, 4A). In addition, the level of antiapoptotic proteins Bcl-2 was significantly decreased on

Molecular Pharmacology Fast Forward. Published on November 29, 2010 as DOI: 10.1124/mol.110.068551
This article has not been copyedited and formatted. The final version may differ from this version.

treatment of LNCaP cells with GL (Fig. 4A). However, expression of Bax proteins was not altered by same treatment of GL in human normal prostate epithelial cell PrEC (Fig. 4B). These results indicated that GL treatment altered ratio of proapoptotic to antiapoptotic Bcl-2 family proteins in LNCaP cells.

Bak and Bax deficiency conferred significant protection against GL-induced apoptosis. Because GL treatment increased the Bax and Bak levels in the cancer cells (Fig. 4A), we hypothesized that these proteins might play an important role in the regulation of GL-induced apoptosis. The SV40-immortalized MEFs derived from WT and DKO mice were selected to test the hypothesis. Because of immortalization by transfection with SV40 genomic DNA, the MEFs cannot be regarded as normal fibroblasts. Initially, we used the MEFs from WT and DKO mice to determine the effect of GL treatment on the cleavage of PARP. Similar to LNCaP cells, GL treatment caused a significant increase in the cleavage of PARP in WT MEFs, but much less in the DKO MEFs (Fig. 4C). The GL treatment caused concentration-dependent and statistically significant inhibition of cell growth, and increase in apoptotic cells in WT MEFs as judged by trypan blue dye exclusion assays (Fig. 4D) and the analysis of cytoplasmic histone-associated DNA fragmentation (Fig. 4E), respectively. On the other hand, the MEFs derived from DKO MEFs mice were significantly more resistant to GL-induced growth inhibition and cytoplasmic histone-associated DNA fragmentation compared with WT MEFs (Fig. 4C-E). Collectively, these results indicated that Bax and Bak play an important role in the execution of GL-induced apoptosis.

GL activated JNKs in human prostate cancer cells but not in PrEC. We, and others, have demonstrated previously that z-Gug-induced apoptosis is regulated by JNKs (Singh et al., 2007; Sarfaraz et al., 2008). However, role of JNK as well as other MAPK kinases, such as p38-

Molecular Pharmacology Fast Forward. Published on November 29, 2010 as DOI: 10.1124/mol.110.068551
This article has not been copyedited and formatted. The final version may differ from this version.

MAPK and ERK in GL-induced apoptosis has not been studied. To elucidate the mechanism of GL-induced apoptosis in human prostate cancer cells, we investigated its effect on MAPKs. The LNCaP (Fig 5A) and C81 cells (results not shown) with 5 μM GL exhibited a rapid but sustained activation of JNK for at least 8 h. JNK phosphorylation in GL-treated LNCaP cells could be detected as early as 2 h (1.4 fold compared the control cells) after treatment, which was not attributable to an increase in total JNK protein level (data not shown). However, the GL treatment did not activate p38 MAPK and ERK kinases (Fig. 5A) or affected their total protein level (data not shown). In addition, 5 μM z-Gug treatment was not found to activate JNK in LNCaP (Fig. 5A) or C81 (data not shown) cells. We raised the question of whether GL-mediated JNK activation was selective for cancer cells. In contrast to prostate cancer cells, GL did not result in the activation of JNK in normal human prostate epithelial cell PrEC (Fig. 5B). The NAC significantly reduced the phospho-c-Jun (Fig. 5C) protein expression by GL in LNCaP cells. These results indicated that JNK activation mediated by ROS may be involved in GL-induced apoptosis that seemed selective towards prostate cancer cells.

GL-mediated activation of Bax was inhibited by ectopic expression of JNKK2(AA). The results shown above indicated critical roles of JNK and Bax activation in GL-induced apoptosis but did not provide any insight into the signaling pathways linking these effects. Next, we questioned if JNK activation contributed to GL-mediated activation of Bax. We addressed this question by determining the effect of ectopic expression of catalytically inactive mutant of JNKK2, which is a JNK-specific upstream kinase (Singh et al., 2007; Chen et al., 1998). GL treatment caused an increase in phosphorylations of JNK and its downstream target c-Jun in the empty-vector transfected LNCaP cells (Fig. 6A). In contrast, GL-mediated hyperphosphorylation of both JNK and c-Jun were fully abolished by ectopic expression of catalytically inactive

Molecular Pharmacology Fast Forward. Published on November 29, 2010 as DOI: 10.1124/mol.110.068551
This article has not been copyedited and formatted. The final version may differ from this version.

JNKK2(AA) in the LNCaP cells (Fig. 6A). In addition, statistically significant increase in cytoplasmic histone-associated DNA fragmentation (6.6 fold of control) resulting from 24 h exposure to GL 5 μM was observed in the empty-vector transfected LNCaP cells but partially and significantly decreased in the cells transiently transfected with JNKK2(AA) (Fig. 6B). Genetic suppression of JNK also attenuated the inhibition of LNCaP cell growth by GL (data not shown). Furthmore, immunoprecipitation analysis of activate Bax from cell lysates was performed by using a monoclonal antibody (6A7) that recognizes an epitope at the N-terminus of the active Bax followed by immunoblotting using polyclonal anti-Bax antibody. The GL treatment caused a remarkable increase in Bax conformational change in the empty-vector transfected LNCaP cells (Fig. 6C). More importantly, overexpression of JNKK2(AA) conferred protection against GL-mediated conformational change of Bax (Fig. 6C). Collectively, these results indicated that the GL-mediated conformational change of Bax was regulated by JNK signaling axis.

However, inhibition of the JNK signaling was not fully protective against the GL-induced cell death (Fig. 6B). Therefore, the roles of the other MAPK signaling such as p38 MAPK and ERK in the apoptosis induction by GL were determined by using the siRNA technology. As can seen in Supplemental Figures. S1 and S2, the protein levels of p38 MAPK and ERK were knocked down ~50% -90% by transient transfection of LNCaP cells with p38 MAPK or ERK-targeted siRNA compared with cells transfected with a control nonspecific siRNA. However, p38 MAPK-siRNA or ERK-siRNA did not have any protection against the apoptotic cell death induced by GL (Figs. S1-2). The data indicate that the GL-induced apoptosis is not mediated by p38 MAPK or ERK.

Molecular Pharmacology Fast Forward. Published on November 29, 2010 as DOI: 10.1124/mol.110.068551
This article has not been copyedited and formatted. The final version may differ from this version.

Moreover, we investigated whether Akt signaling was affected in GL-treated LNCaP cells. Exposure of LNCaP cells to GL resulted in a concentration-dependent and significant inactivation of Akt and its substrate mTOR (Fig. 6D). These results suggested that Akt signaling pathway may be involved in regulation of GL-induced cell death.

Discussion

GL, extract of *Commiphora mukul, has* been safely used for thousands of years in the Indian Ayurvedic medicine practice for treatment of different ailments and has been used recently in many clinical trials focused on its cholesterol-lowering effect (Shishodia et al, 2008; Urizar and Moore, 2003; Badmaev et al., 2003). In the present study, we, for the first time, show that GL has a stronger anti-cancer potential in human prostate cancer cells as evidenced by inhibition of cell growth and induction of apoptotic cell death compared with one of its active constituents (z-Gug). Statistically significant inhibition of cell survival by GL was evident at IC_{50} ~ 1 μmol/L concentrations standardized to z-Gug. The effect on growth inhibition by GL was ~10-fold stronger compared with z-Gug (Fig. 1). Interestingly, a normal prostate epithelial cell line PrEC was significantly more resistant to growth inhibition by GL compared with prostate cancer cells. Based on these results, we conclude that (a) GL treatment decreases survival of human prostate cancer cells irrespective of their androgen-responsiveness, (b) a normal prostate epithelial cell line is significantly more resistant to growth inhibition by GL, and (c) uncharacterized constituent(s) of GL may interact additively or synergistically to inhibit viability of human prostate cancer cells. Even though pharmacokinetic parameters for GL have not been determined in humans, the maximal plasma concentration of z-Gug (C_{max}) in rats was shown to be 3.3- and 18.3 μmol/L following oral gavage with 50 mg z-Gug/Kg body weight and intravenous injection with 18 mg z-Gug/Kg body weight (Verma et al., 1999). Based on these pharmacokinetic

Molecular Pharmacology Fast Forward. Published on November 29, 2010 as DOI: 10.1124/mol.110.068551
This article has not been copyedited and formatted. The final version may differ from this version.

observations, it is possible that the concentrations of GL needed to inhibit cancer cell growth may be achievable in humans. We, more recently (Leeman-Neill et al., 2009) reported that treatment with GL (3 μmol standardized to z-Gug, daily for 3 weeks) resulted in enhancement of cetuximab activity in xenograft model of head and neck cancer.

Apoptosis has emerged as an important mechanism for anticancer effects of many naturally occurring and synthetic agents (Shishodia and Aggarwal, 2004; Samudio et al., 2005; Ichikawa and Aggarwal, 2006; Cheon et al., 2006; Xiao and Singh, 2008; Singh et al., 2007; Xiao and Singh, 2007; Kim et al., 2007; Xiao et al., 2006a-c, 2008, 2009, 2010; Singh et al., 2005a). Our present study indeed indicated that GL inhibits prostate cancer cell viability by causing apoptosis that is characterized by appearance of cytoplasmic histone-associated DNA fragmentation, subdiploid cells, and cleavage of PARP (Fig. 2). In contrast, PrEC is more resistant to apoptosis induction by GL (Fig. 2). These results clearly indicate that antitumor activity of GL against prostate cancer cells is associated with apoptosis induction.

Tumor-specific induction of oxidative stress is expected to offer a powerful therapeutic modality. In fact, many anticancer agents and naturally occurring and synthetic agents exhibit antitumor activity via ROS-dependent activation of apoptotic cell death (Singh et al., 2007; Kim et al., 2007; Xiao et al., 2005b-c, 2006b-c; Fang et al., 2007). The present results indicate that the cell death caused by GL in human prostate cancer cells is triggered by ROS generation. This conclusion is based on following observations: (a) GL treatment caused a dose- and time-dependent ROS production in LNCaP and C81 cells (Fig3. A-B); (b) GL-mediated ROS generation and apoptotic cell death was significantly attenuated by antioxidant NAC (Fig.3D); and (c) same treatment with GL did not affect the ROS induction (Fig. 3C) and cause apoptotic cell death (Fig. 2A-B) in PrEC. It was also reported by us (Singh et al, 2007) that ROS is

Molecular Pharmacology Fast Forward. Published on November 29, 2010 as DOI: 10.1124/mol.110.068551
This article has not been copyedited and formatted. The final version may differ from this version.

indispensable for z-Gug, one of the important active components of GL, caused apoptosis in human prostate cancer PC-3 cells.

The proapoptotic Bcl-2 family proteins, which can be subdivided into the Bax subfamily of multidomain proteins (e.g., Bax and Bak) or BH3-only subfamily (e.g., Bid and Bim), induce mitochondrial membrane permeabilization and release of apoptogenic molecules from mitochondria to the cytosol (Singh et al., 2005a; Xiao et al., 2005b-c). An increase in protein levels of Bax and Bak was observed in GL-treated human prostate cancer cells (Fig. 4A), but not in normal prostate epithelial PrEC cell line (Fig 4B). Furthmone, the SV40-immortalized MEFs derived from Bax- and Bak- DKO mice are statistically significantly more resistant toward GL-induced cell viability and apoptotic cell death compared with MEFs derived from WT mice (Fig. 4C-E). The present study indicates that the multidomain proapoptotic Bcl-2 family members Bax and/or Bak play a critical role in regulation of GL-induced apoptosis. The GL-induced apoptosis in human prostate cancer cells may be exacerbated because of down-regulation of Bcl-2 (Fig 4A). Therefore, further studies are needed to determine the role of antiapoptotic Bcl-2 family members, such as Bcl-2 in regulation of GL-mediated cell death in prostate cancer cells.

The involvement of MAPKs signaling pathways in carcinogenesis and cancer prevention and therapy is well documented (Xiao et al., 2004; 2005a). An interesting observation of the present study is that GL-induced ROS-dependent apoptosis in our model is regulated by JNK signaling axis (Figs. 5 and 6): we show that (a) GL treatment causes a time-dependent JNK activation in human prostate cancer LNCaP (Fig. 5A) and C81 (date not shown) cells; (b) pharmacological inhibition of JNK confers significant protection against GL-mediated apoptosis in LNCaP and C81 cells (data not shown); (c) GL-induced JNK activation, Bax conformational change (activation) and apoptosis induction were observed in empty vector-transfected LNCaP

Molecular Pharmacology Fast Forward. Published on November 29, 2010 as DOI: 10.1124/mol.110.068551
This article has not been copyedited and formatted. The final version may differ from this version.

cells, but were inhibited in the cells after ectopic expression of catalytically inactive mutant of JNKK2 (Fig. 6A-C); and (d). GL treatment could not activate the JNK activation in PrEC (Fig.5B); JNK was reported to regulate Bax translocation through phosphorylation of Bim (Lei and Davis, 2003) and to promote Bax translocation through phosphorylation of 14-3-3 proteins (Tsuruta et al., 2003). Thus, it is reasonable to conclude from the present study that GL-inducted Bax activation is regulated by JNK signaling axis. However, it was reported by Sarfaraz et al. that z-Gug-inhibited skin tumorigenesis in SENCAR mice via inhibition of JNK activation. Further studies are needed to systematically explore the role of JNK activation in GL anticancer potential *in vivo* and other cancers in the future studies. These results indicate also that other MAPK signaling such as p38MAPK and Erk are not but the survival signaling Akt may be a mediator for the apoptotic induced by GL.

In conclusion, the present study reveals that GL is a potent inhibitor of prostate cancer cell growth. The GL-mediated antitumor activity is associated with ROS-dependent apoptotic cell death, and is regulated by JNK signaling axis.

Acknowledgments

We thank the late Dr. Stanley Korsmeyer for the generous gift of MEFs and Dr. Michael Karin for the generous gift of JNKK2(AA) plasmid.

Authorship contributions

D.X. provided oversight for the project, conducted the experiments and wrote the manuscript. Y.Z. performed the experiments. L.P., V.B. and M.M. provided gugulipid and carried out quality control. S.V.S. participated in the research design.

References

Badmaev V, Majeed M, Pacchetti B, and Prakash L (2003) Standardiation of Commiphora Mukul extract in dislipidemia and cardiovascular disease. *NUTRA Foods* **2:** 45-51.

Chao DT and Korsmeyer SJ (1998) BCL-2 family: regulators of cell death. *Annu Rev Immunol* **16***:* 395–419.

Chen CY, Del Gatto-Konczak F, Wu z, and Karin M (1998) Stabilization of interleukin-2 mRNA by the c-Jun NH2-terminal kinase pathway. *Science* **280:** 1945-1949.

Cheon JH, Kim JS, Kim JM, Kim N, Jung HC, and Song IS (2006) Plant sterol guggulsterone inhibits nuclear factor-κB signaling in intestinal epithelial cells by blocking IκB kinase and ameliorates acute murine colitis. *Inflamm Bowel Dis* **12:**1152-1161.

Cui J, Huang L, Zhao A, Lew JL, Yu J, Sahoo S, Meinke PT, Royo I, Pelaez F, and Wright SD (2003) Guggulsterone is a farnesoid X receptor antagonist in coactivator association assays but acts to enhance transcription of bile salt export pump. *J Biol Chem* **278:**10214-10220.

Fang J, Nakamura H, and Lyer AK (2007) Tumaor-targeted induction of oxystress for cancer therapy. *J Drug Target* **15:** 475-486.

Gilligan T, and Kantoff PW (2002) Chemotherapy for prostate cancer. *Urol* **60 (suppl. 3A):** 94-100.

Gujral ML, Sareen K, Tangri KK, Amma MK, and Roy AK (1960) Antiarthritic and anti-inflammatory activity of gum guggul (Balsamodendron mukul Hook). *Ind J Physiol Pharmacol* **4:**267-273.

Ichikawa H and Aggarwal B (2006) Guggulsterone inhibits osteoclastogenesis induced by receptor activator of nuclear factor-κB ligand and by tumor cells by suppressing nuclear factor-κB activation. *Clin Cancer Res* **12:**662-668.

Jemal A, Siegel R, Ward E, How Y, Xu J, and Thun MJ (2009) Cancer Statistics. 2009. *CA Cancer J Clin* **59:** 225-249.

Kim BJ, Ryu SW, and Song BJ (2006) JNK- and p38 kinase-mediated phosphorylation of Bax leads to its activation and mitochondrial translocation and to apoptosis of human hepatoma HepG2 cells. *J Biol Chem* **281:** 21256-21265.

Kim YA, Xiao D, Xiao H, Powolny AA, Lew KL, Reilly ML, Zeng Y, Wang Z, and Singh SV (2007) Mitochondria-mediated apoptosis by diallyl trisulfide in human prostate cancer cells is associated with generation of reactive oxygen species and regulated by Bax/Bak. *Mol. Cancer Ther* **6:**1599-1609.

Leeman-Neill RJ, Wheeler SE, Singh SV, Thomas SM, Seethala RR, Neill DB, Panahanden MC, Hahm ER, Joyce SC, Sen M, et al. (2009) Guggulsterone enhances head and neck cancer therapies viainhibition of signal transducer and activator of transcription-3. *Carcinegesis* **11:** 1848-1856.

Lei K and Davis RJ (2003) JNK phosphorylation of Bim-related members of the Bcl2 family induces Bax-dependent apoptosis. *PNAS* **100:** 2432–2437.

Samudio I, Konopleva M, Safe S, McQueen T, and Andreeff M (2005) Guggulsterone induce apoptosis and differentiation in acute myeloid leukemia: identification of isomer-specific antileukemic activities of the pregnadienedione structure. *Mol Cancer Ther* **4:**1982-1992.

Sarfaraz S, Siddiqui IA, Syed DN, Afaq F, and Mukhtar H (2008) Guggulsterone modulates MAPK and NF-κB pathways and inhibits skin tumorigenesis in SENCAR mice. *Carcinogenesis* **29:** 2011-2018.

Shishodia S and Aggarwal BB (2004) Guggulsterone inhibits NF-kappaB and IkappaBalpha kinase activation, suppresses expression of anti-apoptotic gene products, and enhances apoptosis. *J Biol Chem* **279:**47148-47158.

Shishodia S, Harikumar KB, Dass S, Ramawat KG, and Aggarwal BB (2008) The guggul for chronic disease: ancient medicine, modern targets. *Anticancer Res* **28:** 3647-3664.

Sinal CJ and Gonzalez FJ (2002) Guggulsterone: an old approach to a new problem. *Trends Endocrinol Metab* **13:**275-276.

Singh SV, Choi S, Zeng Y, Hahm ER, and Xiao D (2007) Guggulsterone-induced apoptosis in human prostate cancer cells is caused by reactive oxygen intermediate-dependent activation of c-Jun NH_2-terminal kinase**.** *Cancer Res* **67:**7439-7449.

Singh SV, Srivastava SK, Choi S, Lew KL, Antosiewicz J, Xiao D, Zeng Y, Watkins SC, Johnson CS, Trump DL, Leey J, Xiao H, and Herman-Antosiewicz A (2005a Sulforaphane-induced cell death in human prostate cancer cells is initiated by reactive oxygen species. *J Biol Chem* **280:** 19911-19924.

Singh SV, Zeng Y, Xiao D, Vogel VG, Nelson JB, Dhir R, and Tripathi YB (2005b Caspase-dependent apoptosis induction by guggulsterone, a constituent of Ayurvedic medicinal plant *Commiphora mukul*, in PC-3 human prostate cancer cells is mediated by Bax and Bak. *Mol Cancer Ther* **4:**1747-1754.

Tsuruta F, Sunayama J, Mori Y, Hatt6ori S, Shimizu S, Tsujjmoto Y, Yoshioka K, Masuyama N, and Gotoh Y (2003) JNK promotes Bax translocation to mitochondria through phosphorylation of 14-3-3 proteins. *EMBO J* **23:** 1889–1899.

Urizar NL, Liverman AB, Dodds DT, Silv FV, Ordentlich P, Yan Y, Gonzaleg FJ, Heyman RA, Mangelsdorf DJ, and Moore DD (2002) A natural product that lowers cholesterol as an antagonist ligand for FXR. *Science* **296:**1703-1706.

Urizar NL and Moore DD (2003) GUGULIPID: a natural cholesterol-lowering agent. *Annu Rev Nutr* **23:**303-313.

Verma N, Singh SK, and Gupta RC (1999) Pharmacokinetics of guggulsterone after intravenous and oral administration in rats. *Pharm Pharmacol Comm* **5:** 349-354.

Whittemore AS, Kolonel LN, Wu AH, John EM, Gallagher RP, Howe GR, Burch JD, Hankin J, Dreon DM, West DW, et al. (1995) Prostate cancer in relation to diet, physical activity, and body size in blacks, whites and Asians in the United States and Canada. *J. Natl. Cancer Ins* **87:** 652-661.

Wu J, Xia C, Meier J, Li S, Hu X, and Lala DS (2002) The hypolipidemic natural product guggulsterone acts as an antagonist of the bile acid receptor. *Mol Endocrinol* **16:**1590-1597.

Xiao D, Choi S, Johnson DE, Vogel VG, Johnson CS, Trump DL, Lee YJ, and Singh SV (2004) Diallyl trisulfide-induced apoptosis in human prostate cancer cells involves c-Jun N-terminal kinase and extracellular-signal regulated kinase-mediated phosphorylation of Bcl-2.*Oncogene* **23:**5594-5606.

Xiao D, Choi S, Lee YJ, and Singh SV (2005a) Role of mitogen-activated protein kinases in phenethyl isothiocyanate-induced apoptosis in human prostate cancer cells. Mol *Carcinogenesis* **43:** 130-140.

Xiao D, Herman-Antosiewicz A, Antosiewicz J, Xiao H, Brisson M, Lazo JS, and Singh SV (2005b Diallyl trisulfide-induced G_2-M phase cell cycle arrest in human prostate cancer cells is caused by reactive oxygen species-dependent destruction and hyperphosphorylation of Cdc25C. *Oncogene* **24:** 6256-6268.

Xiao D, Lew KL, Kim YA, Zeng Y, Hahm ER, Dhir R, and Singh SV (2006a) Diallyl trisulfide suppresses growth of PC-3 human prostate cancer xenograft *in vivo* in association with Bax and Bak induction. *Clin Cancer Res* **12:** 6836-6843.

Xiao D, Lew KL, Zeng Y, Xiao H, Marynowski SW, Dhir R, and Singh SV (2006b) Phenethyl isothiocyanate-induced apoptosis in PC-3 human prostate cancer cells is mediated by reactive oxygen species-dependent disruption of the mitochondrial membrane potential. *Carcinogenesis* **27:** 2223-2234.

Xiao D, Powolny AA**,** Antosiewicz J, Hahm ER, Bommareddy A, Zeng Y, Desai D, Amin S, Herman-Antosiewicz A, and Singh SV (2009) Cellular responses to dietary cancer chemopreventive agent D,L-sulforaphane in human prostate cancer cells are initiated by mitochondria-derived reactive oxygen species. *Pharm Res* **26:**1729-1738.

Xiao D**,** Powolny AA, and Singh SV (2008) Benzyl isothiocyanate targets mitochondrial respiratory chain to trigger reactive oxygen species-dependent apoptosis in human breast cancer cells. *J Biol Chem* **283**: 30151-30163.

Xiao D and Singh SV (2010) P66Shc is indispensable for phenethyl isothiocyanate-induced apoptosis in human prostate cancer cells. *Cancer Res* **70:**3150-3158.

Xiao D and Singh SV (2008) Guggulsterone, a constituent of Indian Ayurvedic medicinal plant *Commiphora mukul*, inhibits angiogenesis *in vitro* and *in vivo*. *Mol.Cancer Ther* **7:** 171-180.

Xiao D and Singh SV (2007) Phenethyl isothiocyanate inhibits angiogenesis *in vitro* and *ex vivo*. *Cancer Res* **67:** 2239-2246.

Xiao D, Vogel V and Singh SV (2006c) Benzyl isothiocyanate-induced cell death in MDA-MB-231 and MCF-7 human breast cancer cells is initiated by reactive oxygen species and regulated by Bax and Bak. *Mol.Cancer Ther* **5:**2931-2945.

Xiao D, Zeng Y, Choi S, Lew KL, Nelson JB, and Singh SV (2005c Caspase-dependent apoptosis induction by phenethyl isothiocyanate, a cruciferous vegetable-derived cancer chemopreventive agent, is mediated by bak and bax. *Clin Cancer Res* **11:**2670-2679.

Footnotes

This work was supported by the National Institutes of Health National Cancer Institute [grant R21-CA143104 (DX)].

Molecular Pharmacology Fast Forward. Published on November 29, 2010 as DOI: 10.1124/mol.110.068551
This article has not been copyedited and formatted. The final version may differ from this version.

FIGURE LEGENDS

Figure 1. Effect of GL (GL contains ~3.75% z-Gug and was standardized to z-Gug (μM), A, B and D) and z-Gug (C) on survival of LNCaP, C81 and PrEC cells determined by the colonogenic assay (A) and trypan blue dye exclusion assay (B-D). Cells were treated with different concentrations of GL or z-Gug for 24 h. *Columns,* mean of three determinations; *bars,* SE. *Significantly different ($P < 0.05$) compared with DMSO-treated control by one-way ANOVA followed by Dunnett's test. Similar results were observed in two independent experiments. Representative data from a single experiment are shown.

Figure 2. GL induced apoptosis in LNCaP and C81 cells, but not in normal human prostate epithelial cells PrEC, determined by (A) quantitation of cytoplasmic histone associated DNA fragmentation, (B) flow cytomitry analysis of Sub-G0/G1 cell phase, and (C) immunoblotting cleavage of PARP. Cells were treated with the indicated concentrations of GL or DMSO (control) for 24 Hours. Results in panels A and B are expressed as enrichment factor relative to cells treated with DMSO (control). Results are mean ± SE (n= 3). *Significantly different (P<0.05) between the indicated groups by one-way ANOVA followed by by Dunnett's test. In panel C, the cleaved PARP by immunoblotting using lysates from GL-treated or DMSO-treated LNCaP and C81 cells. The blot was stripped and re-probed with anti-α-Tubulin antibody to ensure equal protein loading. Similar results were observed in at least two independent experiments. Representative data from a single experiment are shown.

Figure 3. GL-induced ROS production was involved in apoptotic cell death caused by GL. GL caused ROS generation in C81 (A) and LNCaP (B) cells in dose- (left panel of A for C81) and

Molecular Pharmacology Fast Forward. Published on November 29, 2010 as DOI: 10.1124/mol.110.068551
This article has not been copyedited and formatted. The final version may differ from this version.

time- (right panel of A for C81 and B for LNCaP) dependent manner, but not in PrEC (C). (D) NAC protected against GL-mediated ROS production and apoptosis. LNCaP cells were treated with 10 mM NAC for 2 h, and then exposed to 5μM GL standardized to z-Gug for 30 min (left panel of D) or 24 h (right panel of D). In panels A- D, results are mean ± SE (*n*= 3). *Significantly different (*P*<0.05) between the indicated groups by one-way ANOVA followed by Dunnett's test (left panel of A and C) and Bonferroni's multiple comparison test (D), and by paired t-test (right panel of A and B. Experiments were repeated twice with triplicate measurements in each experiment. The results were consistent and representative data from a single experiment are shown.

Figure 4. A, Immunoblotting for Bax, Bak, and Bcl-2 proteins using lysates from LNCaP cells treated with DMSO (control) or 5 μmol/L GL standardized to z-Gug for the indicated time periods. **B,** Immunoblotting for Bax protein using lysates from PrEC treated with DMSO (control) or 5 μmol/L GL standardized to z-Gug for the indicated time periods. **C**, Immuniblotting for cleaved PARP protein from the SV 40-immoratalized mouse embryonic fibroblasts derived –Wild Tipe (WT) and Bax and Bak double knockout mice treated with DMSO (control) or 2.5 and 5 μmol/L GL standardized to z-Gug for 24 h. For **A - C**, the blots were stripped and re-probed with anti-actin antibody to normalize for differences in protein level. The numbers on top of the immunoreactive bands represent change in protein levels relative to DMSO-treated cells. Immunoblotting for each protein was performed at least twice using independently prepared lysates. **D,** the cell survival and **E,** cytoplasmic histone-associated DNA fragmentation in LNCaP cells treated with DMSO (control) or 2.5 and 5 μmol/L GL standardized to z-Gug for 24 h. For **D** and **E**, *Columns,* mean (*n*= 3); *bars,* SE. *Significantly different (*P*

<0.05) compared with corresponding DMSO treated control by one-way ANOVA followed by Dunnett's test. Each experiment was performed at least twice with triplicate measurements in each experiment. The results were consistent and representative data from a single experiment are shown.

Figure 5. The GL treatment increased activating phosphorylation of c-Jun N-terminal kinase (JNK) in LNCaP cells, but not in PrEC. **A**, Immunoblotting for phospho-JNK, phosphor-Erk and phospho-p38 MAPK using lysates from LNCaP cells and B, Immunoblotting for phospho-JNK using lysates from PrEC treated with DMSO (control) or 5 μM GL standardized to z-Gug or 5 μM z-Gug for the indicated time periods. The blots were stripped and re-probed with anti-actin antibody to ensure equal protein loading. Immunoblotting for each protein was performed twice using independently prepared lysates and the results were similar. Representative data from a single experiment are shown. Fold change in phospho/total protein level relative to DMSO-treated control at each time point is shown on top of the immunoreactive band. **C**, NAC protected against GL-mediated JNK activation. LNCaP cells were treated with 10 mM NAC for 2 h, and then with or without 2.5 μM GL standardized to z-Gug for 8 h. The cellular lysates from these groups were performed for immunoblotting of phospho-c-Jun. The blots were stripped and re-probed with anti-actin antibody to ensure equal protein loading. The numbers on top of the immunoreactive bands represent change in protein levels relative to corresponding DMSO-treated control. Immunoblotting for the protein was performed twice using independently prepared lysates and the results were similar. Representative data from a single experiment are shown.

Molecular Pharmacology Fast Forward. Published on November 29, 2010 as DOI: 10.1124/mol.110.068551
This article has not been copyedited and formatted. The final version may differ from this version.

Figure 6. A, immunoblotting for phospho-JNK and phospho-c-Jun using lysates from LNCaP cells transiently transfected with the empty pcDNA3.1 vector or pcDNA3.1 vector encoding catalytically inactive mutant of JNKK2 [JNKK2(AA)] and treated for 8 h with DMSO (control) or 5 μM GL. B**,** cytoplasmic histone-associated DNA fragmentation in LNCaP cells transiently transfected with the empty pcDNA3.1 vector or pcDNA3.1 vector encoding JNKK2(AA) and treated for 24 h with DMSO (control) or 5 μM GL. Results are mean ± SE (n= 3). *Significantly different (P<0.05) between the indicated groups by one-way ANOVA followed by Bonferroni's multiple comparison test. **C,** analysis of conformational change of Bax using lysates from LNCaP cells transiently transfected with the empty pcDNA3.1 vector or pcDNA3.1 vector encoding JNKK2(AA) and treated for 8 h with DMSO (control) or 5 μM GL. Bax protein was immunoprecipitated from equal amounts of lysate proteins using ant-Bax 6A7 monoclonal antibody. The immunoprecipitated complexes were subjected to immunoblotting using anti-Bax polyclonal antibody. D, Immunoblotting for Akt, S473phosphor-Akt and S2448phospho-mTOR proteins using lysates from LNCaP cells treated with DMSO (control) or indicated concentrations of GL standardized to z-Gug for 24 h. For **A** and **D**, the blots were stripped and re-probed with anti-actin antibody to ensure equal protein loading. The numbers on top of the immunoreactive bands represent change in protein levels relative to corresponding DMSO-treated control. Each experiment was repeated twice with comparable results. Representative data from a single experiment are shown.

Figure 1

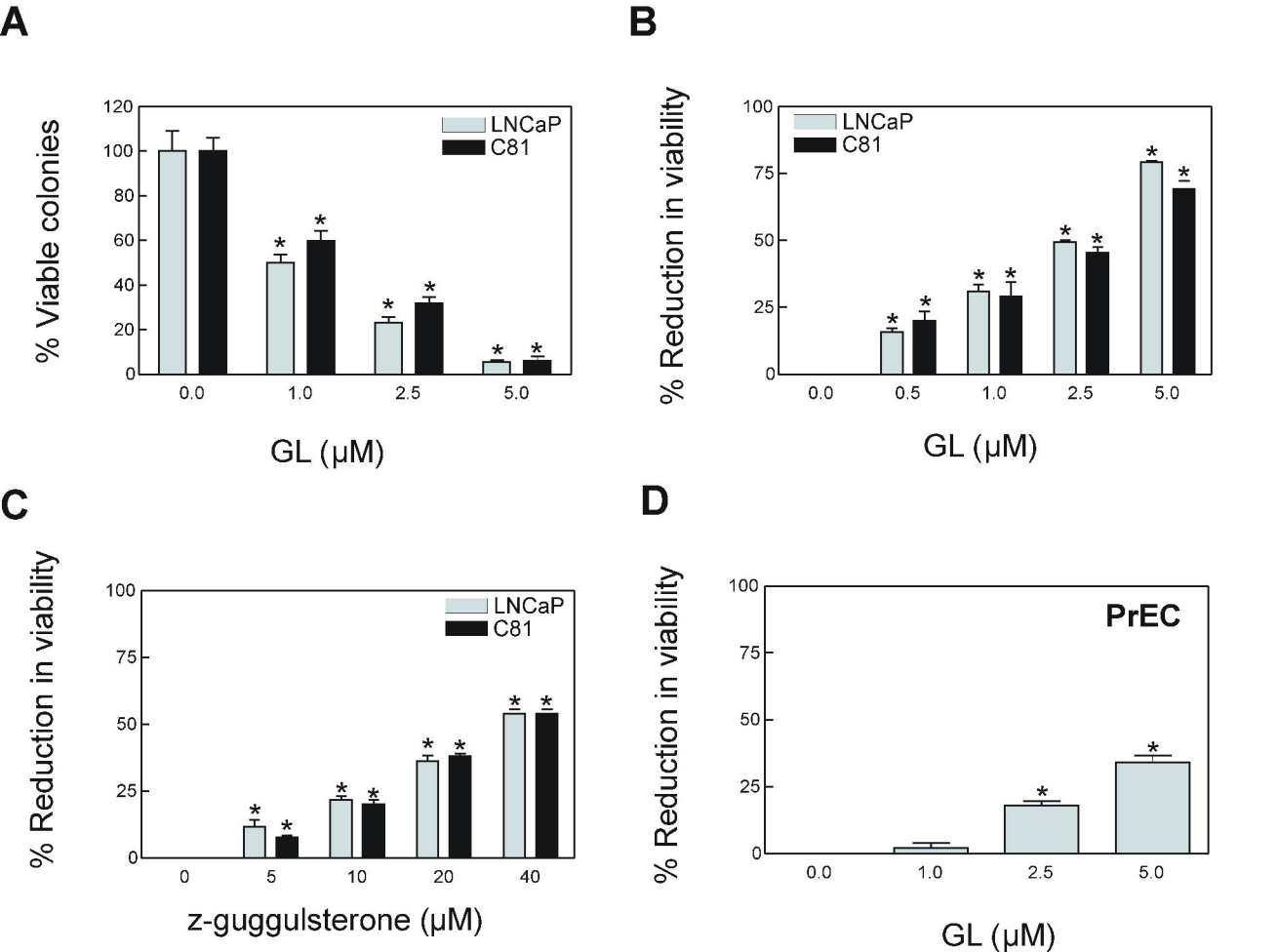
A
% Viable colonies
120
100
80
60
40
20
0
LNCaP
C81
0.0
1.0
2.5
5.0
GL (μM)
B
% Reduction in viability
100
75
50
25
0
LNCaP
C81
0.0
0.5
1.0
2.5
5.0
GL (μM)
C
% Reduction in viability
100
75
50
25
0
LNCaP
C81
0
5
10
20
40
z-guggulsterone (μM)
D
% Reduction in viability
100
75
50
25
0
PrEC
0.0
1.0
2.5
5.0
GL (μM)

Figure 2

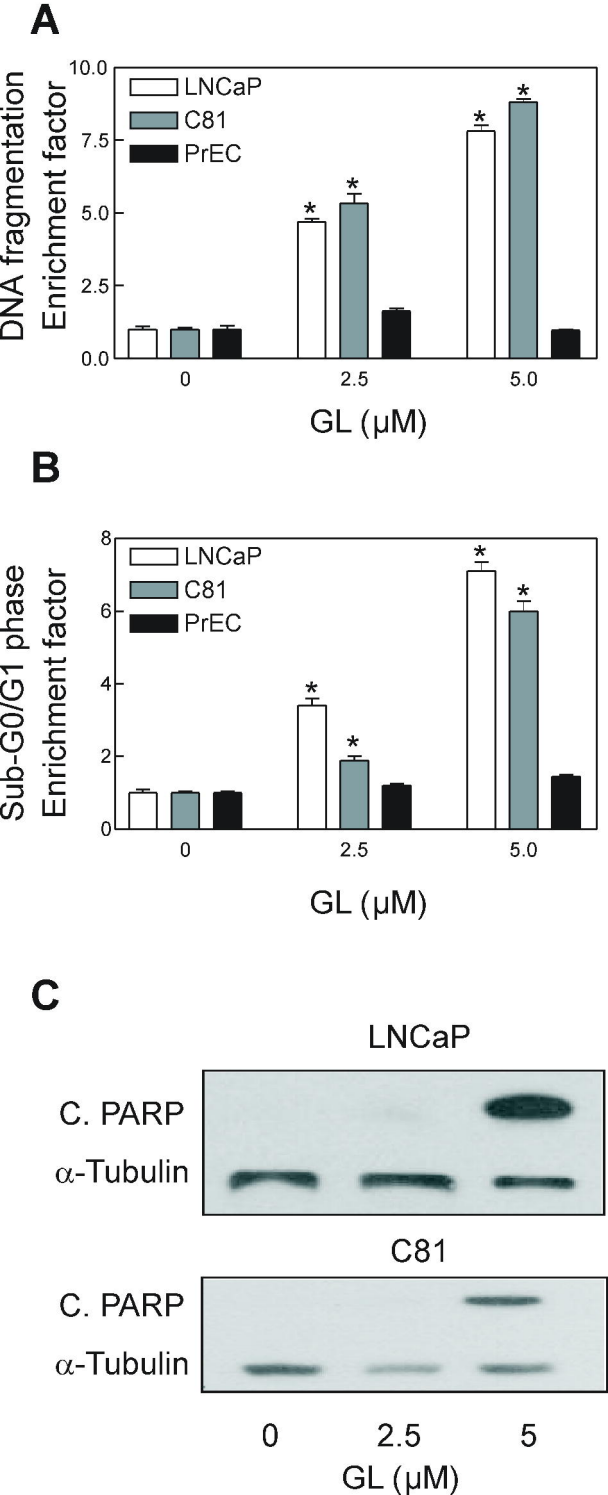
A
DNA fragmentation
Enrichment factor
10.0
7.5
5.0
2.5
0.0
LNCaP
C81
PrEC
*
0
2.5
5.0
GL (μM)
B
Sub-G0/G1 phase
Enrichment factor
8
6
4
2
0
LNCaP
C81
PrEC
*
0
2.5
5.0
GL (μM)
C
LNCaP
C. PARP
α-Tubulin
C81
C. PARP
α-Tubulin
0
2.5
5
GL (μM)

Figure 3

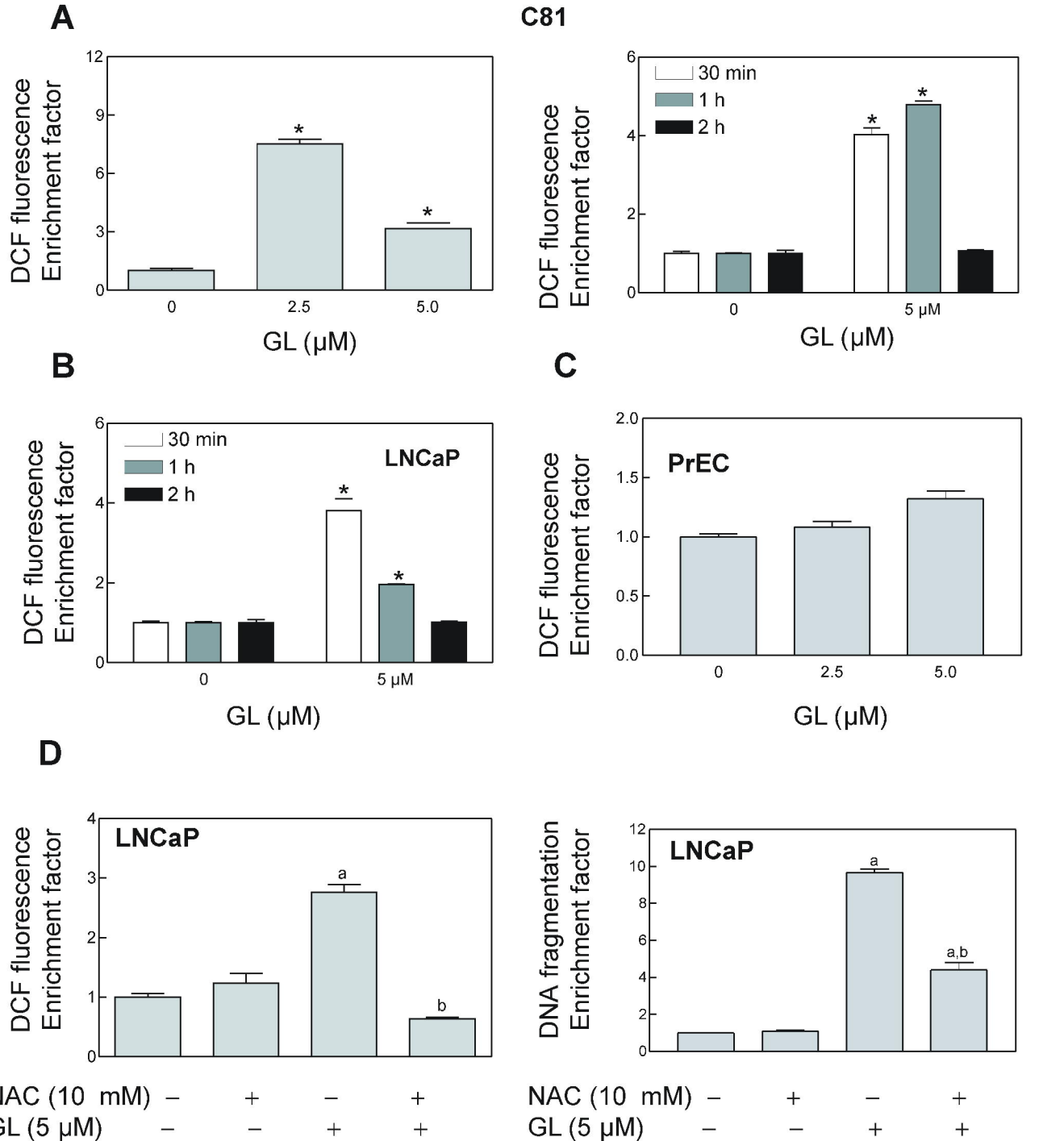
A
C81
DCF fluorescence
Enrichment factor
12
9
6
3
0
*
*
0
2.5
5.0
GL (μM)
6
4
2
0
30 min
1 h
2 h
*
*
0
5 μM
GL (μM)
B
6
4
2
0
30 min
1 h
2 h
LNCaP
*
*
0
5 μM
GL (μM)
C
2.0
1.5
1.0
0.5
0.0
PrEC
0
2.5
5.0
GL (μM)
D
4
3
2
1
0
LNCaP
a
b
NAC (10 mM) – + – +
GL (5 μM) – – + +
DNA fragmentation
Enrichment factor
12
10
8
6
4
2
0
LNCaP
a
a,b
NAC (10 mM) – + – +
GL (5 μM) – – + +

Figure 4

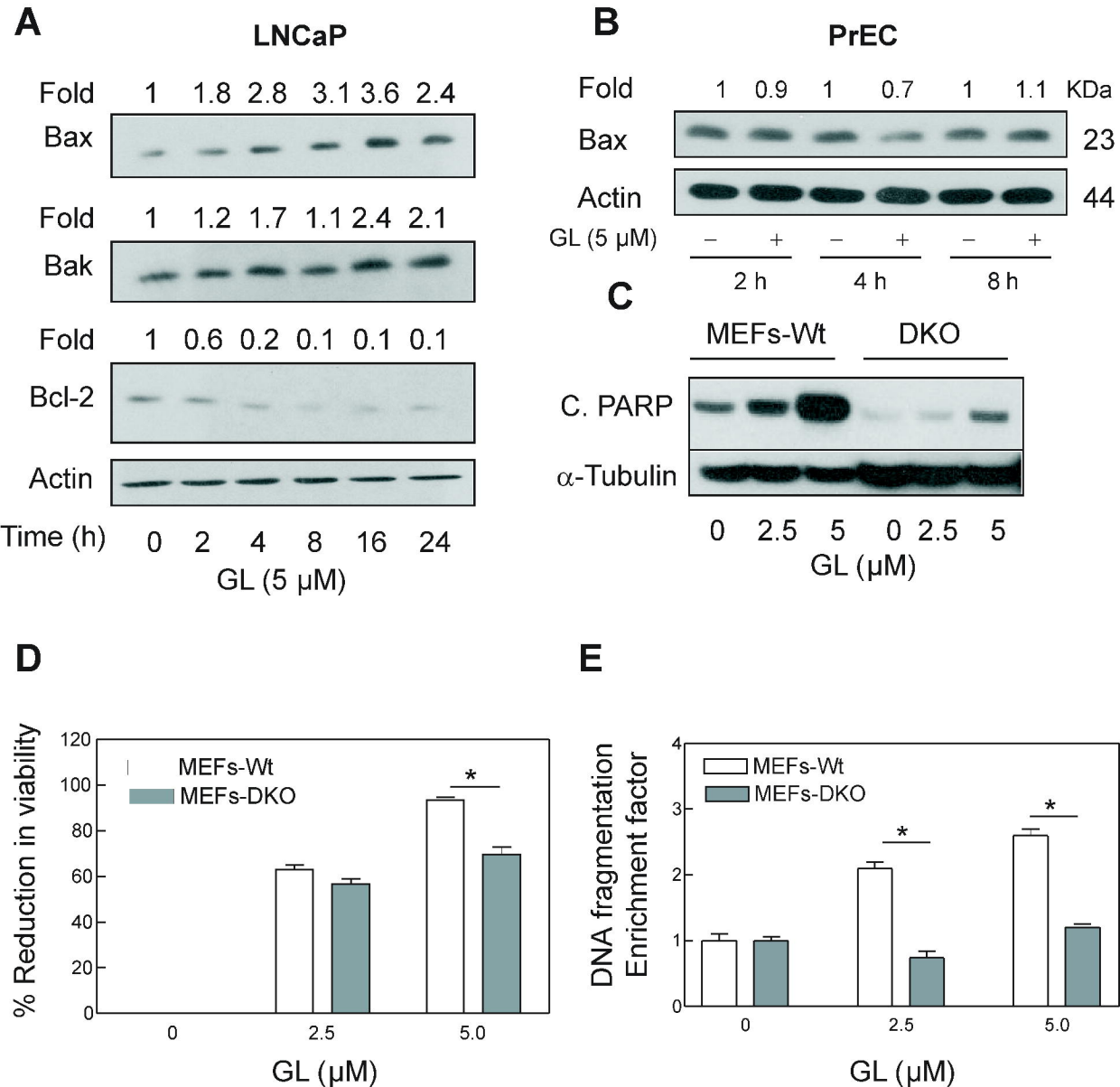
A
LNCaP
Fold 1 1.8 2.8 3.1 3.6 2.4
Bax
Fold 1 1.2 1.7 1.1 2.4 2.1
Bak
Fold 1 0.6 0.2 0.1 0.1 0.1
Bcl-2
Actin
Time (h) 0 2 4 8 16 24
GL (5 μM)
B
PrEC
Fold 1 0.9 1 0.7 1 1.1 KDa
Bax 23
Actin 44
GL (5 μM) – + – + – +
2 h 4 h 8 h
C
MEFs-Wt DKO
C. PARP
α-Tubulin
0 2.5 5 0 2.5 5
GL (μM)
D
% Reduction in viability
MEFs-Wt
MEFs-DKO
120
100
80
60
40
20
0
*
0 2.5 5.0
GL (μM)
E
DNA fragmentation Enrichment factor
MEFs-Wt
MEFs-DKO
4
3
2
1
0
* *
0 2.5 5.0
GL (μM)

Figure 5

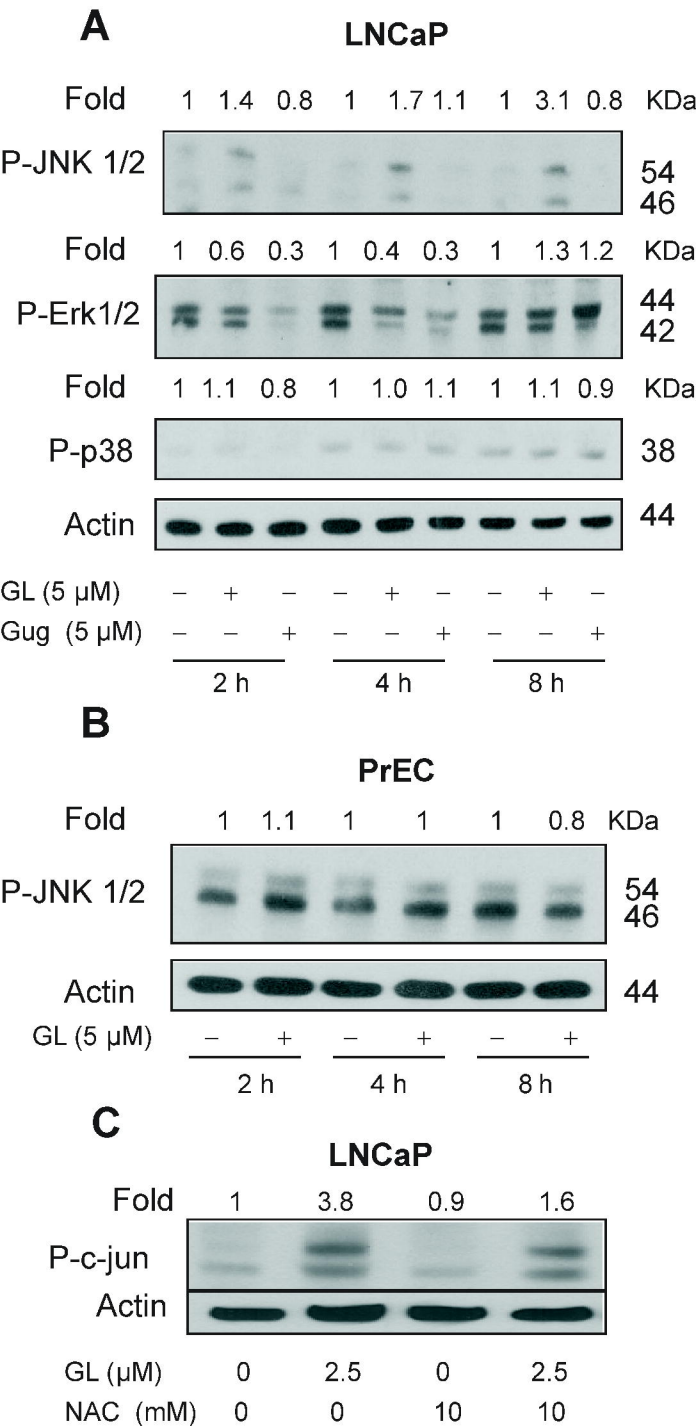
A
LNCaP
Fold 1 1.4 0.8 1 1.7 1.1 1 3.1 0.8 KDa
P-JNK 1/2
54
46
Fold 1 0.6 0.3 1 0.4 0.3 1 1.3 1.2 KDa
P-Erk1/2
44
42
Fold 1 1.1 0.8 1 1.0 1.1 1 1.1 0.9 KDa
P-p38
38
Actin
44
GL (5 μM) – + – – + – – + –
Gug (5 μM) – – + – – + – – +
2 h
4 h
8 h
B
PrEC
Fold 1 1.1 1 1 1 0.8 KDa
P-JNK 1/2
54
46
Actin
44
GL (5 μM) – + – + – +
2 h
4 h
8 h
C
LNCaP
Fold 1 3.8 0.9 1.6
P-c-jun
Actin
GL (μM) 0 2.5 0 2.5
NAC (mM) 0 0 10 10

Figure 6

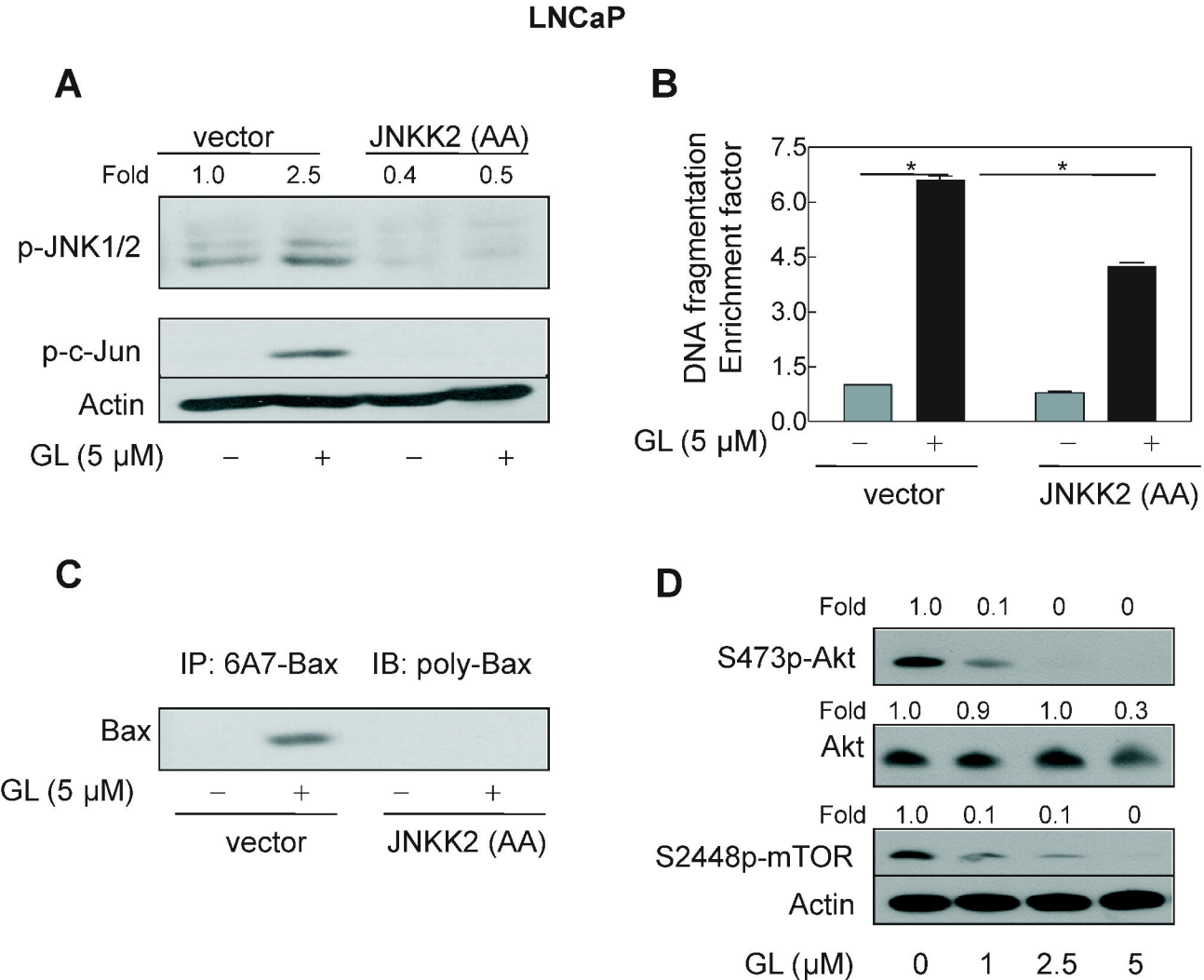
LNCaP
A
vector
JNKK2 (AA)
Fold
1.0
2.5
0.4
0.5
p-JNK1/2
p-c-Jun
Actin
GL (5 μM)
–
+
–
+
B
DNA fragmentation
Enrichment factor
7.5
6.0
4.5
3.0
1.5
0.0
*
*
GL (5 μM)
–
+
–
+
vector
JNKK2 (AA)
C
IP: 6A7-Bax
IB: poly-Bax
Bax
GL (5 μM)
–
+
–
+
vector
JNKK2 (AA)
D
Fold
1.0
0.1
0
0
S473p-Akt
Fold
1.0
0.9
1.0
0.3
Akt
Fold
1.0
0.1
0.1
0
S2448p-mTOR
Actin
GL (μM)
0
1
2.5
5